Int. J. Adv. Appl. Math. and Mech. 3(3) (2016) 19 – 26 (ISSN: 2347-2529)

Journal homepage: www.ijaamm.com

IJAAMM

International Journal of Advances in Applied Mathematics and Mechanics

Effect of radiation and chemical reaction on an unsteady Walter's-B viscoelastic MHD flow past a vertical porous plate

Research Article

N. Pandya, A. K. Shukla*

Department of mathematics and astronomy, University of Lucknow, Lucknow-226007, India

Received 06 October 2015; accepted (in revised version) 26 December 2015

Abstract: This paper investigates study of unsteady Walter's-B viscoelastic MHD (magnetohydrodynamics) flow past a vertical porous plate embedded in porous medium with the effects of radiation and chemical reaction. Dimensionless partial differential equations of governing equations of flow are solved numerically using Crank-Nicolson finite difference method. Velocity, Temperature and Concentration profiles are discussed through graphs for different values of parameters. Skin-friction coefficients, Nusselt number and Sherwood number are discussed through tables for different values of parameters.

MSC: 76W05 • 76R50 • 78A40 • 76M20 • 80A32

Keywords: MHD • Chemical reaction • Thermal radiation • Porous medium • Heat and mass transfer • Crank-Nicolson method

1. Introduction

From last many decades, large number of mathematician have been attracted towards investigation of unsteady MHD flow of Non-Newtonian fluid because study of heat and mass transfer in Non-Newtonian fluid has application in different field of engineering and science like milk processing, chemical and process engineering, blood oxygenators, mixing mechanisms and dissolution process etc.

There exist many viscoelastic fluids and their models to study Non-Newtonian fluids like second grade viscoelastic fluids, third grade viscoelastic fluids, micropolar fluids, Rivlin Ericksen model, Maxwell model and Walter's-B model etc.

The watlter's-B model or viscoelastic fluids had been developed to simulate accurately tribiological, biotechnological and many complex polymeric viscous fluid possessing short time elastic effects. Steady flow and heat transfer of WalterâĂŹs-B model viscoelastic fluid between two parallel uniformly porous disk rotating about common axis was analyzed by Rath et al.[1]. Takhar [2]investigated flat plate thermal convection boundary layer low of a Walter's-B fluid using numerical shooting quadrature. Jain et al. [3] studied the Hall effect and cross flow effect on free and forced Walter's-B viscoelastic convection flow with radiation. Pravin et al.[4] got exact solution for the combined non similar MHD flow heat and mass transfer phenomena in a conducting viscoelastic Walter's-B fluid percolating a porous regime adjacent to a stretching sheet with heat generation, viscous dissipation and wall mass flux effect using confluent hypergeometric functions for different thermal boundary conditions at the wall.

Dholey et al. [5] analyzed the steady two dimensional stagnation point flow of a walter's-B fluid along a flat deformable stretching surface. Ganesan et al.[6]examined transient free convective flow past a semi infinite vertical flat plate with mass transfer by using Crank-Nicolson finite difference method. Pandya and Shukla[7] studied Soret-Dufour and radiation effects on unsteady MHD flow past an inclined porous plate with variable temperature and mass transfer. Pandya and Shukla[8] Soret-Dufour and radiation with viscous dissipation on unsteady MHD flow over an

* Corresponding author.
E-mail addresses: ashishshukla1987@gmail.com (A. K. Shukla)

inclined porous plate embedded in porous medium. Vishwanath et al.[9]studied the effects of radiation on unsteady free convection heat and mass transfer in a Walter's-B viscoelastic flow past an impulsively started vertical plate.

Hence the objective of this paper is to analyze the effects of radiation and chemical reaction on unsteady Walter's-B viscoelastic MHD flow past a semi infinite vertical plate. Non-dimensional form of partial differential equations of flow has been solved by applying Crank-Nicolson implicit finite difference method. Velocity, temperature and concentration profiles are discussed through graphs for different values of parameters. Skin friction coefficient, Nusselt number and Sherwood number has been discussed through tables.

2. Mathematical analysis

An unsteady flow of a viscoelastic incompressible electrically conducting fluid past an impulsively started infinite vertical porous plate with variable temperature and variable mass diffusion with radiation are analyzed. Plate is embedded in porous medium, x'-axis and y'-axis is taken along and normal to plate respectively. Initially the plate and fluid are at the same temperature and concentration T'_∞ and C'_∞ respectively. At time $t' > 0$ plate is given in motion along x' direction with constant velocity u_0. A transverse magnetic field B_0 is considered normal to the direction of flow. Magnetic Reynold number and transversely applied magnetic field are very small, therefore induced magnetic field is negligible [10].

Due to infinite length in x' direction the flow variables are functions of y' and t' only. Under the above assumptions, the governing boundary layer equations with Boussinesq's approximation are

Continuity equation:

$$\frac{\partial v'}{\partial y'} = 0 \Rightarrow v' = -v_0(constant) \tag{1}$$

Momentum equation:

$$\begin{aligned}\frac{\partial u'}{\partial t'} + v'\frac{\partial u'}{\partial y'} = \nu\frac{\partial^2 u'}{\partial y'^2} - k_0\frac{\partial^3 u'}{\partial y'^2 \partial t'} + g\beta(T' - T'_\infty)cos(\alpha) \\ + g\beta^*(C' - C'_\infty)cos(\alpha) - \frac{\sigma B_0^2 u'}{\rho} - \frac{\nu u'}{K'}\end{aligned} \tag{2}$$

Energy equation:

$$\rho C_p\left(\frac{\partial T'}{\partial t'} + v'\frac{\partial T'}{\partial y'}\right) = k\frac{\partial^2 T'}{\partial y'^2} - \frac{\partial q_r}{\partial y'} \tag{3}$$

Equation of continuity for mass transfer:

$$\frac{\partial C'}{\partial t'} + v'\frac{\partial C'}{\partial y'} = D\frac{\partial^2 C'}{\partial y'^2} - k_r(C' - C'_\infty) \tag{4}$$

where g is gravitational acceleration, β is the volumetric coefficient of thermal expansion, β^* is the coefficient of volume expansion for mass transfer, K' is the permeability of porous medium, σ is the electrical conductivity of the fluid, T' is the dimensional temperature, ν is the kinematic viscosity, μ is viscosity, ρ is the fluid density, B_0 is magnetic induction, q_r is radiative heat flux in y'-direction, D is mass diffusion coefficient, k_r is chemical reaction rate constant, k_0 Walter's-B viscoelasticity parameter, c_p is specific heat at constant pressure, k is the thermal conductivity of the fluid.

Initial and Boundary conditions are given as:

$$\begin{cases} t' \le 0 \quad u' = 0 \quad T' = T'_\infty \quad C' = C'_\infty \quad \forall y' \\ t' > 0 \quad u' = u_0 \quad v' = -v_0 \quad T' = T'_\infty + (T'_w - T'_\infty)e^{At'}, \\ C' = C'_\infty + (C'_w - C'_\infty)e^{At'} \quad at\ y' = 0 \\ u' = 0 \quad T' \to \infty \quad C' \to \infty \quad y' \to \infty \end{cases} \tag{5}$$

where, $A = \dfrac{v_0^2}{\nu}$, T'_w and C'_w are tmeperature and concentration of plate respectively.

Radiative heat flux term using the Roseland approximation is given by

$$q_r = -\frac{4\sigma}{3k_m}\frac{\partial T'^4}{\partial y'} \tag{6}$$

where σ and k_m are Stefan Boltzmann constant and mean absorption coefficient respectively. It is considered that the temperature difference within the flow are sufficiently small such that T'^4 may be expressed as a linear function of the temperature. This is accomplished by expanding in a Taylor series about T'_∞ and neglecting the higher order terms,

thus

$$T'^4 \cong 4T_\infty'^3 T' - 3T_\infty'^4 \tag{7}$$

then using Eqs. (6) and (7), Eq. (3) is reduced

$$\rho C_p\left(\frac{\partial T'}{\partial t'} + v'\frac{\partial T'}{\partial y'}\right) = k\frac{\partial^2 T'}{\partial y'^2} + \frac{16\sigma T_\infty'^3}{3k_l}\frac{\partial^2 T'}{\partial y'^2} \tag{8}$$

In order to acquire non-dimensional partial differential equations, introducing following dimensionless quantities:

$$\begin{cases} u = \frac{u'}{u_0},\ y = \frac{y'v_0}{\nu},\ t = \frac{t'v_0^2}{\nu},\ \theta = \frac{T'-T'_\infty}{T'_w-T'_\infty},\ \Gamma = \frac{k_0 v_0^2}{\nu^2} \\ C = \frac{C'-C'_\infty}{C'_w-C'_\infty},\ Gm = \frac{\nu g\beta^*(C'_w-C'_\infty)}{u_0 v_0^2}, Gr = \frac{\nu g\beta(T'_w-T'_\infty)}{u_0 v_0^2},\ K_r = \frac{k_r\lambda}{v_0^2} \\ K = \frac{v_0^2 K'}{\nu^2},\ Pr = \frac{\mu c_p}{k},\ M = \frac{\sigma B_0^2 \nu}{\rho v_0^2},\ R = \frac{4\sigma T_\infty'^3}{k_l k},\ Sc = \frac{\nu}{D} \end{cases} \tag{9}$$

By virtue of Eq. (9), we get non-dimensional form of Eqs. (2), (3) and (8) respectively:

$$\frac{\partial u}{\partial t} - \frac{\partial u}{\partial y} = \frac{\partial^2 u}{\partial y^2} - \Gamma\frac{\partial^3 u}{\partial y^2 \partial t} + Gr\,\theta + Gm\,C - \left(M + \frac{1}{K}\right)u \tag{10}$$

$$\frac{\partial \theta}{\partial t} - \frac{\partial \theta}{\partial y} = \frac{1}{Pr}\left(1 + \frac{4R}{3}\right)\frac{\partial^2 \theta}{\partial y^2} \tag{11}$$

$$\frac{\partial C}{\partial t} - \frac{\partial C}{\partial y} = \frac{1}{Sc}\frac{\partial^2 C}{\partial y^2} - K_r C \tag{12}$$

with following initial and boundary conditions in non-dimensional form are:

$$\begin{cases} t \le 0 \quad u = 0 \quad \theta = 0 \quad C = 0 \quad \forall\, y \\ t > 0 \quad u = 1 \quad \theta = e^t \quad C = e^t \quad at\ y = 0 \\ u = 0 \quad u \to 0 \quad C \to 0 \quad y \to 0 \end{cases} \tag{13}$$

Now, many research workers have interest to calculate physical quantities skin-friction coefficients τ along wall x-axis, Nusselt number Nu and Sherwood number Sh.
Non-dimensional form of these physical quantities are:

$$\begin{cases} \tau = \left(\frac{\partial u}{\partial y}\right)_{y=0} \\ Nu = -\left(\frac{\partial \theta}{\partial y}\right)_{y=0} \\ Sh = -\left(\frac{\partial C}{\partial y}\right)_{y=0} \end{cases} \tag{14}$$

3. Method of solution

System of non-linear partial differential Eqs. (10)-(12) are solved using boundary and initial conditions (13). In this case, exact solution is not possible. Therefore we solve these equations by Crank-Nicolson implicit finite difference method to obtain numerical solution. Equivalent finite difference scheme of Eqs. (10)-(12) are as follows:

$$\begin{aligned} \frac{u_{i,j+1}-u_{i,j}}{\Delta t} - \frac{u_{i+1,j}-u_{i,j}}{\Delta y} &= \left(\frac{u_{i-1,j}-2u_{i,j}+u_{i+1,j}+u_{i-1,j+1}-2u_{i,j+1}+u_{i+1,j+1}}{2(\Delta y)^2}\right) \\ &\quad + Gr\left(\frac{\theta_{i,j+1}-\theta_{i,j}}{2}\right) + Gm\left(\frac{C_{i,j+1}-C_{i,j}}{2}\right) \\ -\left(M+\frac{1}{K}\right)\left(\frac{u_{i,j+1}+u_{i,j}}{2}\right) - \Gamma\left(\frac{u_{i-1,j}-2u_{i,j}+u_{i+1,j}+u_{i-1,j+1}-2u_{i,j+1}+u_{i+1,j+1}}{2(\Delta y)^2\Delta t}\right) & \end{aligned} \tag{15}$$

$$\begin{aligned} \frac{\theta_{i,j+1}-\theta_{i,j}}{\Delta t} - \frac{\theta_{i+1,j}-\theta_{i,j}}{\Delta y} &= \\ \frac{1}{Pr}\left(1+\frac{4R}{3}\right)\left(\frac{\theta_{i-1,j}-2\theta_{i,j}+\theta_{i+1,j}+\theta_{i-1,j+1}-2\theta_{i,j+1}+\theta_{i+1,j+1}}{2(\Delta y)^2}\right) & \end{aligned} \tag{16}$$

$$\frac{C_{i,j+1}-C_{i,j}}{\Delta t}-\frac{C_{i+1,j}-C_{i,j}}{\Delta y}=\frac{1}{Sc}\left(\frac{C_{i-1,j}-2C_{i,j}+C_{i+1,j}+C_{i-1,j+1}-2C_{i,j+1}+C_{i+1,j+1}}{2(\Delta y)^2}\right) -K_r\left(\frac{C_{i,j+1}-C_{i,j}}{2}\right) \tag{17}$$

corresponding boundary and initial conditions are also exressed as

$$\begin{cases} u_{i,0}=0 \quad \theta_{i,0}=0 \quad C_{i,0}=0 \quad \forall\, i \\ u_{0,j}=1 \quad \theta_{0,j}=e^{j\Delta t} \quad C_{0,j}=e^{j\Delta t} \\ u_{X,j}=0 \quad \theta_{X,j}\to 0 \quad C_{X,j}\to 0 \end{cases} \tag{18}$$

Here index i refers to y, j refers to time t, $\Delta t=t_{j+1}-t_j$ and $\Delta y=y_{i+1}-y_i$. Knowing the values of u, θ and C at time t , we can compute the values at time $t+\Delta t$ as follows: we substitute $i=1,2,...,L-1$, where L correspond to ∞, in Eqs. (15)-(17) which make up tridiagonal system of equations, can be figured out by Thomas algorithm as discussed in Carnahan et al.[11]. Subsequently θ and C are known for all values of y at time $t+\Delta t$. Replace these values of and in Eq. (15) and solved by same procedure with initial and boundary condition, we obtain solution for u till desired time t .

The implicit Crank-Nicolson finite difference method is a second order method $\left(o\left(\Delta t^2+\Delta y^2\right)\right)$ in time and has no restriction on space and time steps, that is, the method is unconditionally stable. The computation is executed for $\Delta y=0.1$, $\Delta t=0.001$ and procedure is repeated till $y=4$.

4. Result and discussion

In order to get a physical insight into the problem, a representative set of numerical results is shown graphically in figures to illustrate the influence of physical parameters.

In Fig. 1, velocity profile decreases as chemical reaction parameter Kr increases. Similarly in Fig. 2 concentration profile decreases when Kr increases. To illustrate the effects of Prandtl number Pr on velocity u and temperature θ on increasing Pr, clearly velocity profile u and temperature profile θ decreases strongly in Figs. 7 and 8 respectively.

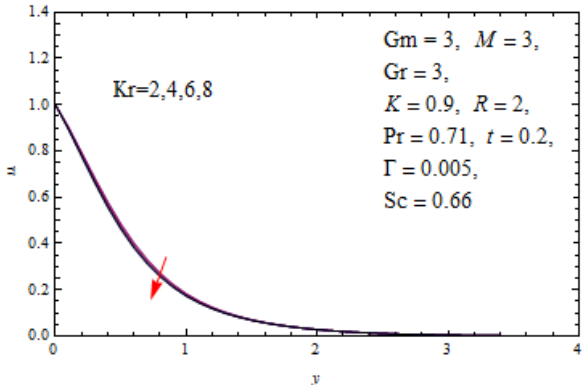

Fig. 1. Velocity Profile for Different Values of Kr

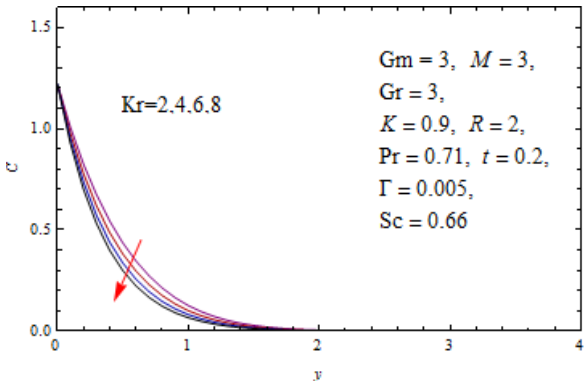

Fig. 2. Concentration Profile for Different Values of Kr

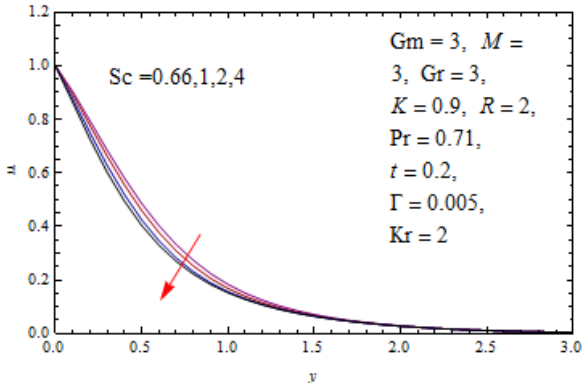

Fig. 3. Velocity Profile for Different Values of Sc

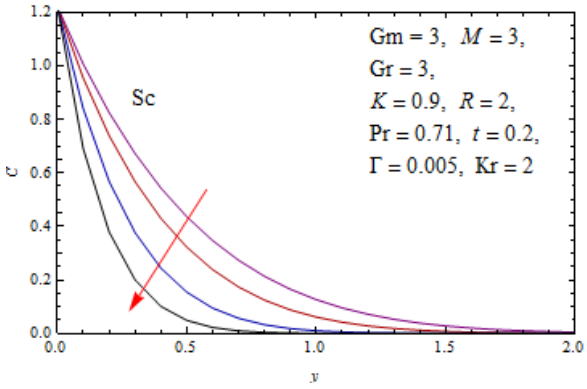

Fig. 4. Concentration Profile for Different Values of Sc

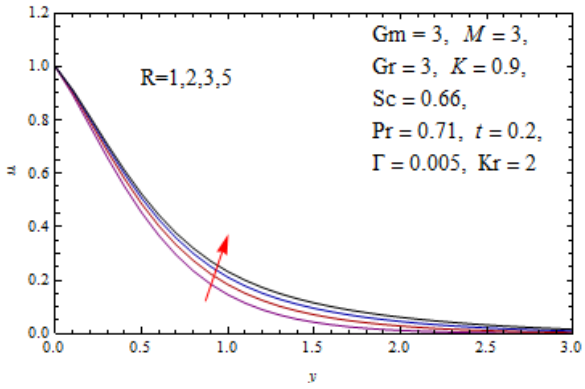

Fig. 5. Velocity Profile for Different Values of R

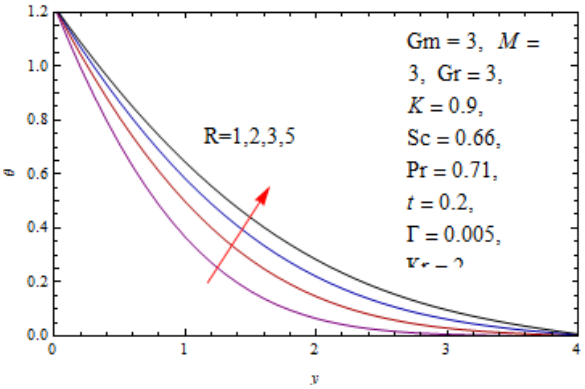

Fig. 6. Temperature Profile for Different Values of R

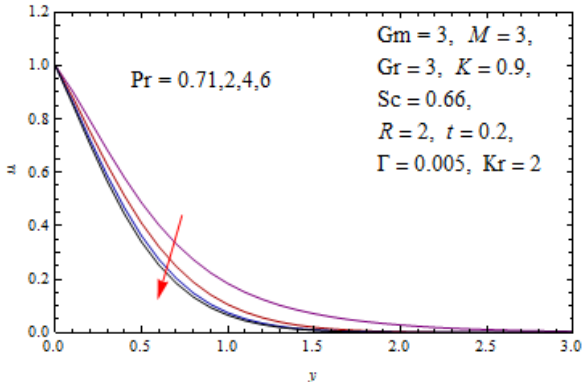

Fig. 7. Velocity Profile for Different Values of Pr

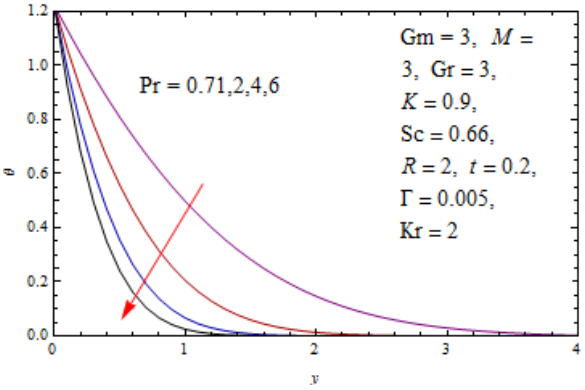

Fig. 8. Temperature Profile for Different Values of Pr

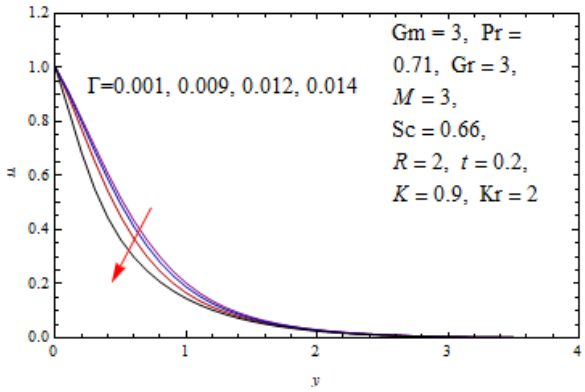

Fig. 9. Velocity Profile for Different Values of Γ

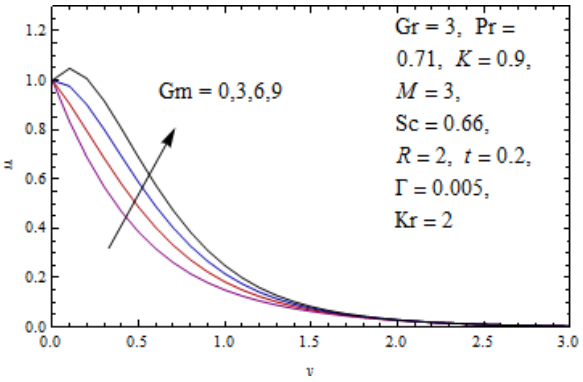

Fig. 10. Velocity Profile for Different Values of Gm

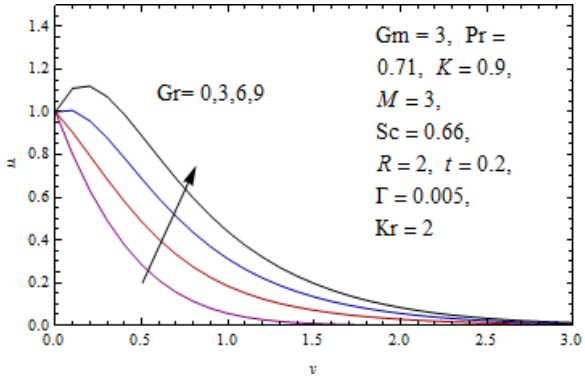

Fig. 11. Velocity Profile for Different Values of Gr

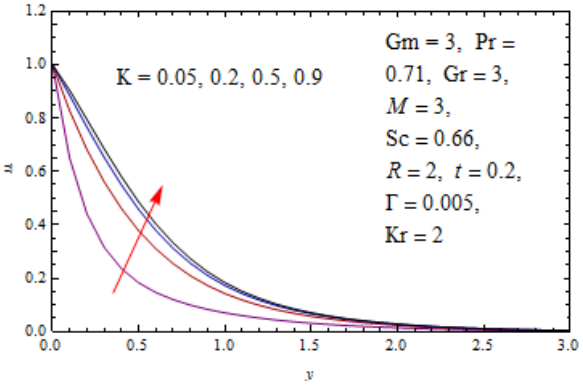

Fig. 12. Velocity Profile for Different Values of K

Table 1. Skin friction coefficient for different values of parameters

Γ	Kr	K	M	Pr	R	Sc	Gm	Gr	t	τ
0.001	2	0.9	3	0.71	2	0.66	3	3	0.2	−0.889345
0.009	2	0.9	3	0.71	2	0.66	3	3	0.2	−1.07028
0.012	2	0.9	3	0.71	2	0.66	3	3	0.2	−1.20061
0.016	2	0.9	3	0.71	2	0.66	3	3	0.2	−1.55838
0.005	2	0.9	3	0.71	2	0.66	0	3	0.2	−1.68252
0.005	2	0.9	3	0.71	2	0.66	6	3	0.2	−0.2409
0.005	2	0.9	3	0.71	2	0.66	9	3	0.2	0.479911
0.005	2	0.9	3	0.71	2	0.66	3	0	0.2	−1.99371
0.005	2	0.9	3	0.71	2	0.66	3	3	0.2	0.0702845
0.005	2	0.9	3	0.71	2	0.66	3	9	0.2	1.10228
0.005	2	0.05	3	0.71	2	0.66	3	3	0.2	−3.50737
0.005	2	0.2	3	0.71	2	0.66	3	3	0.2	−1.72787
0.005	2	0.5	3	0.71	2	0.66	3	3	0.2	−1.15532
0.005	4	0.9	3	0.71	2	0.66	3	3	0.2	−1.00118
0.005	6	0.9	3	0.71	2	0.66	3	3	0.2	−1.03579
0.005	8	0.9	3	0.71	2	0.66	3	3	0.2	−1.06637
0.005	2	0.9	1	0.71	2	0.66	3	3	0.2	−0.47668
0.005	2	0.9	6	0.71	2	0.66	3	3	0.2	−1.56992
0.005	2	0.9	9	0.71	2	0.66	3	3	0.2	−2.06979
0.005	2	0.9	3	2	2	0.66	3	3	0.2	−1.18278
0.005	2	0.9	3	4	2	0.66	3	3	0.2	−1.34844
0.005	2	0.9	3	6	2	0.66	3	3	0.2	−1.44618
0.005	2	0.9	3	0.71	1	0.66	3	3	0.2	−1.05279
0.005	2	0.9	3	0.71	3	0.66	3	3	0.2	−0.904841
0.005	2	0.9	3	0.71	4	0.66	3	3	0.2	−0.864716
0.005	2	0.9	3	0.71	2	1	3	3	0.2	−1.06019
0.005	2	0.9	3	0.71	2	2	3	3	0.2	−1.22104
0.005	2	0.9	3	0.71	2	4	3	3	0.2	−1.36511
0.005	2	0.9	3	0.71	2	0.66	3	3	0.1	−1.85632
0.005	2	0.9	3	0.71	2	0.66	3	3	0.3	−0.4098
0.005	2	0.9	3	0.71	2	0.66	3	3	0.4	−0.0418052

Table 2. Nusselt number for different values of parameters

Γ	Kr	K	M	Pr	R	Sc	Gm	Gr	t	τ
0.005	2	0.9	3	2	2	0.66	3	3	0.2	1.6179
0.005	2	0.9	3	4	2	0.66	3	3	0.2	2.39077
0.005	2	0.9	3	6	2	0.66	3	3	0.2	2.99738
0.005	2	0.9	3	0.71	1	0.66	3	3	0.2	1.16711
0.005	2	0.9	3	0.71	3	0.66	3	3	0.2	0.767494
0.005	2	0.9	3	0.71	4	0.66	3	3	0.2	0.675243
0.005	2	0.9	3	0.71	2	0.66	3	3	0.1	1.0408
0.005	2	0.9	3	0.71	2	0.66	3	3	0.3	0.89938
0.005	2	0.9	3	0.71	2	0.66	3	3	0.4	0.931792

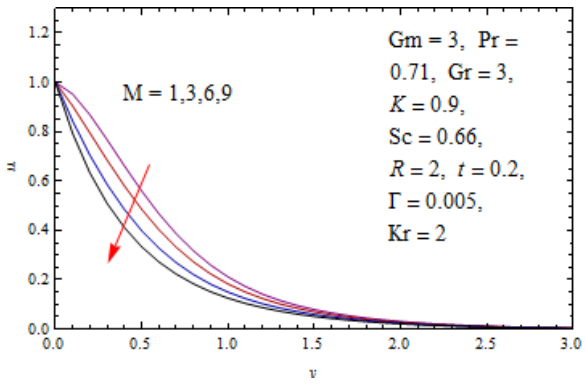

Fig. 13. Velocity Profile for Different Values of M

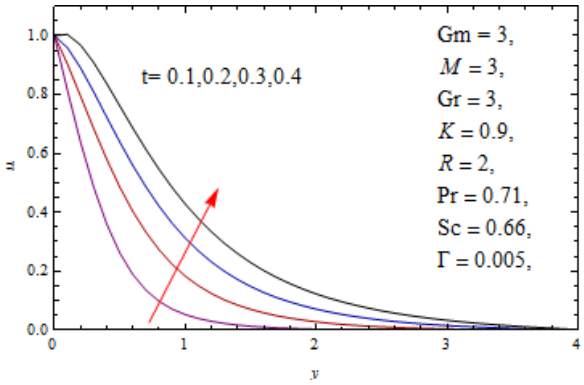

Fig. 14. Velocity Profile for Different Values of t

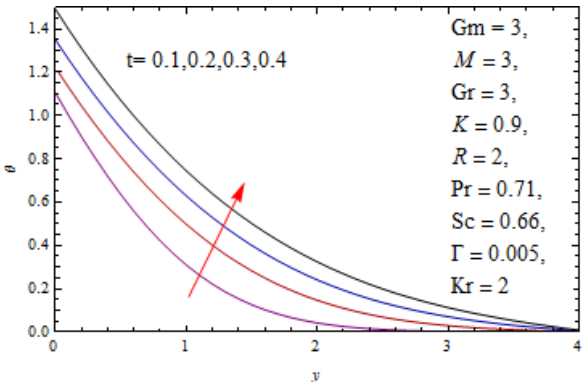

Fig. 15. Temperature Profile for Different Values of t

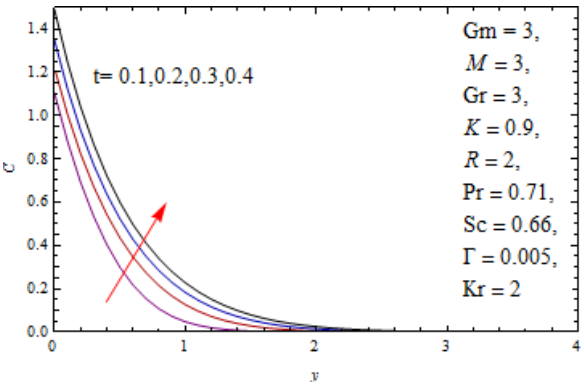

Fig. 16. Concentration Profile for Different Values of t

Table 3. Sherwood number for different values of parameters

Γ	Kr	K	M	Pr	R	Sc	Gm	Gr	t	τ
0.005	4	0.9	3	0.71	2	0.66	3	3	0.2	2.44767
0.005	6	0.9	3	0.71	2	0.66	3	3	0.2	2.71451
0.005	8	0.9	3	0.71	2	0.66	3	3	0.2	2.9531
0.005	2	0.9	3	0.71	2	1	3	3	0.2	2.67125
0.005	2	0.9	3	0.71	2	2	3	3	0.2	3.81353
0.005	2	0.9	3	0.71	2	4	3	3	0.2	5.30397
0.005	2	0.9	3	0.71	2	0.66	3	3	0.1	2.2303
0.005	2	0.9	3	0.71	2	0.66	3	3	0.3	2.25933
0.005	2	0.9	3	0.71	2	0.66	3	3	0.4	2.44319

Velocity profile u and concentration profile C decreases weakly and strongly in Figs. 3 and 4 respectively as Schmidt number Sc increases. On increasing Magnetic parameter M, velocity profile u decreases in Fig. 13 strongly near wall regime and velocity profile u decreases in Fig. 12 strongly near fall regime as permeability of porous medium K increases. Fig. 11 and Fig. 10 depict that on increasing thermal Grashof number Gr and solutal Grashof number Gm , velocity profile u increases strongly. It is analyzed in Figs. 5 and Fig. 6 that on increasing radiation parameter R, velocity profiles increases strongly far-field regime of boundary layer and temperature profile θ increase strongly respectively. It is of great interest to show how the time t effects on velocity, temperature and concentration. It is observed that velocity profile u increases strongly far field regime in Fig. 14, temperature profile θ increases strongly near and far field regime in Fig. 15 and concentration profile increases near wall regime in Fig. 16 when time t increases. Fig. 9 depicts that on increasing viscoelastic parameter Γ, velocity profile decreases near wall regime.

Table 1 depicts that on increasing viscoelasticity parameter Γ, chemical reaction parameter Kr, Magnetic parameter M, Prandtl number Pr and Schmidt number Sc, skin friction coefficient τ decreases. On the other hand on increasing solutal Grashof number Gm, thermal Grashof number Gr, permeability of porous medium K, radiation parameter R and time t, skin friction coefficient τ increases.

It is analyzed in Table 3 that Kr and Sc increase, Sherwood number Sh increases while Sh first decreases after then increases as time t increases. Table 2 shows that on increasing Pr and R Nusselt number Nu increases and decreases respectively. Nu first decreases after then increases as time t increases.

5. Conclusion

A two dimensional unsteady Walter's-B viscoelastic MHD flow past a vertical porous plate embedded in porous medium with radiation and chemical reaction effects has been presented. The dimensionless system of partial differential equations of flow field are solved with implicit Crank-Nicolson finite difference numerical method. The present computations have analyzed that increasing viscoelasticity deaccelerates the velocity.
On increasing Schmidt number Sc, Sherwood number Sh increases and skin friction coefficient τ decreases. On increasing Prandtl number Pr, Nusselt number Nu increases while skin friction coefficient τ decreases. Skin friction coefficient τ decreases when viscoelasticity increases.

Acknowledgements

We acknowledge the U.G.C. (University Grant Commission) and thank for providing financial support for the research work. We are also thankful to different software companies (Mathematica, MatLab and LaTeX) for developing the techniques that help in the computation and editing.

References

[1] R. S. Rath, S. N. Bastia, Steady low and heat transfer in a viscoelastic fluid between two coaxial rotating disk, Proc. Mathematical Sciences. 87(8) (1978) 227–236.
[2] H. S. Takhar, A. A. Raptis, Heat transfer from flow of an elastico-viscous fluid, Int Comm. Heat and Mass Trasnfer. 16(2)(1989) 193–197.
[3] P. Jain, R. C. Chaudhary, Hall effect on MHD mixed convection flow of a viscoelastic fluid past an infinite vertical porous plate with mass transfer and radiation, Theoretical and Applied Mechanics. 33(4) (2006) 281–309.
[4] V. K. Pravin, P. H. Veena, K. Rajgopal, Non similar solutions for heat and mass transfer flow in an electrically conducting viscoelastic fluid over a streching sheet saturated in a porous medium with suchtion/blowing, J. Porous Media. 11(2) (2008) 219–230.
[5] S. Dholey. T Ray Mahapatra, A. S. Gupta, Momentum and heat transfer in the magnetohydrodynamics stagnation point flow of a viscoelastic fluid towards a streching surfaces , Mechanica. 42(3) (2007) 263–272.
[6] P. Ganesan, V. M. Soundalgekar, Finite difference analysis of transient free convection with mass transfer on an isothermal vertical flat plate, Int. J. of Eng. Sciences. 9 (1981) 757–770.
[7] N. Pandya, A. K. Shukla, Soret-Dufour and radiation effects on unsteady MHD flow past an impulsively started inclined porous plate with variable temperature and mass diffusion, Int. J. of Math. and Sci. Comp. 3(2) (2013) 41–48.
[8] N. Pandya, A. K. Shukla, Soret-Dufour and radiation effects on unsteady MHD flow over an inclined porous plate embedded in porous medium with viscous dissipation, Int. J, Adv. Appl. Math. and Mech. 2(1) (2014) 107–119.
[9] G. Vishwanath, V. Ramchandra Prasad, B. Vasu, V Rajeshvara Rao, Radiation effects on unsteady free convection heat and mass transfer in a Walter's-B viscoelastic flow past an impulsively started vertical plate, Int. J. of Scie. and Eng. R. 3(8) (2012) 1–9.
[10] T. G. Cowling, Magnetohydrodynamics, Intersicence Publisher. Newyork, 1957.
[11] Brice Carnahan, H. A. Luthor, J. O. Wilkes, Applied Numerical Methods, John Wiley and Sons. New York, 1969.